Exploring the Lower Limit in Hydrogen Bonds: Analysis of Weak C−H···O and C−H···π Interactions in Substituted Coumarins from Charge Density Analysis

ARTICLE *in* THE JOURNAL OF PHYSICAL CHEMISTRY A · MARCH 2005

Impact Factor: 2.69 · DOI: 10.1021/jp046388s · Source: PubMed

2 AUTHORS, INCLUDING:

Parthapratim Munshi
Shiv Nadar University
42 PUBLICATIONS **659** CITATIONS

SEE PROFILE

Exploring the Lower Limit in Hydrogen Bonds: Analysis of Weak C−H···O and C−H···π Interactions in Substituted Coumarins from Charge Density Analysis

Parthapratim Munshi and Tayur N. Guru Row*

Solid State and Structural Chemistry Unit, Indian Institute of Science, Bangalore-560012, India

Received: August 11, 2004; In Final Form: October 27, 2004

Experimental electron densities in coumarin, 1-thiocoumarin, and 3-acetylcoumarin have been analyzed based on the X-ray diffraction data at 90 K. These compounds pack in the crystal lattice with weak C−H···O and C−H···π interactions, and variations in charge density properties and derived local energy densities have been investigated in the regions of intermolecular interactions. Theoretical charge density calculations on crystals using the B3LYP/6-31G** method show remarkable agreement with the derived properties and energy densities from the experiment. The intermolecular interactions follow an exponential dependence of electron density and energy densities at the bond critical points. The Laplacian follows a "Morse-like" dependence on the length of the interaction line. Based on the set of criteria defined using the theory of "atoms in molecules", it has become possible to distinguish between a hydrogen bond (C−H···O) and a van der Waals interaction (C−H···π). This has resulted in the identification of a "region of overlap" in terms of electron densities, energy densities, and mutual penetration of the hydrogen and acceptor atoms with respect to the interaction length. This approach suggests a possible tool to distinguish between the two types of interactions.

Introduction

An accurate experimental measurement and analysis of charge density in a molecular crystal can be obtained from high-resolution X-ray diffraction data at low temperatures.[1] The nature of chemical interactions can be evaluated in terms of the deformation densities.[2,3] To account for the deformation densities due to chemical bonding, several algorithms have been developed. The commonly used approach for this purpose is the Hansen−Coppens formalism[4] in which the individual atomic densities are divided into three components: the core, spherical expansion, and contraction term (κ) in the valence shell and the valence deformation in terms of density normalized spherical harmonics ($d_{lm\pm}$), together with the corresponding radial expansion and contraction (κ') of the valence shell as given below,

$$\rho_{\mathrm{at}}(\mathbf{r}) = P_c\rho_{\mathrm{core}}(\mathbf{r}) + P_v\kappa^3\rho_{\mathrm{valence}}(\kappa\mathbf{r}) + \sum_{l=0}^{l_{\max}}\kappa'^3 R_l(\kappa'\mathbf{r})\sum_{m=0}^{l} P_{lm\pm}d_{lm\pm}(\vartheta,\varphi)$$

The electron density in the crystal is modeled based on this $\rho(\mathbf{r})$ as a sum of atom centered charge distributions

$$\rho(\mathbf{r}) = \sum_j \rho_j(r_j)$$

Bader's quantum theory of "atoms in molecules" (AIM) approach[5,6] allows for the interpretation of the charge density obtained from experimental electron density as derived from the above methodology. It also provides a pathway for comparing the experimental electron density with theoretically derived density in terms of topological properties of the density $\rho(\mathbf{r})$. The topology of the charge density manifests as local maxima at the positions of the nuclei and the features can be analyzed with the AIM approach. In general, the theory of AIM provides a methodology for the identification of a bond between any two atoms in a molecule. This analysis is based on the identification of critical points, classified using the Hessian matrix of the electron density.[5,7] The line of the highest electron density linking any two atoms is referred to as the "bond path" and its length R_{ij} (need not be the same as interatomic vector) is referred to as the "interaction line". The bond critical points (BCPs) lie along the bond path with the gradient of the electron density, $\Delta\rho_b(\mathbf{r}) = 0$. The second derivative of the electron density, the *Laplacian* $\nabla^2\rho_b(\mathbf{r})$ ($=\sum_{i=1}^{3}\lambda_i,\lambda_i$ are the curvatures of a bond at the BCP) represents the chemical features of the molecules. If $\nabla^2\rho_b(\mathbf{r}) < 0$, the density is locally concentrated resulting in shared interactions, while in the case of $\nabla^2\rho_b(\mathbf{r}) > 0$ the electron density is depleted representing closed-shell interactions. The bond paths, interaction lines, and the Laplacian values together represent the topology of the charge density distribution in a given molecule. Thus the AIM approach could be used for both theoretical and experimental analysis.

The topological analysis, however, does not specify the character of the bond but only indicates the existence of a bond. To characterize a bond in terms of its chemical concepts, such as bond order, ionicity conjugation, and hydrogen bonding, the properties evaluated at the BCPs become crucial. Koch and Popelier have proposed eight criteria to establish hydrogen bonding in particular, which allows to distinguish a hydrogen bond from a van der Waals interaction.[7,8] If one or more of these criteria are not satisfied the concerned interaction can be considered as van der Waals interaction. Among these eight criteria the fourth condition is considered as necessary and sufficient to fully describe a hydrogen bond. The first condition is the presence of a BCP between a donor atom and an acceptor atom linked via a bond path. The second condition is the presence of charge density evaluated at the BCP and its relationship with the overall hydrogen bond energy. It is possible

* Corresponding author. Tel: +91-80-22932796, +91-80-22932336. Fax +91-80-23601310. E-mail: ssctng@sscu.iisc.ernet.in

10.1021/jp046388s CCC: $30.25
Published on Web 12/10/2004

TABLE 1: Experimental X-ray Data

compound formula	coumarin	1-thiocoumarin	3-acetylcoumarin
	$C_9H_6O_2$	C_9H_6OS	$C_{11}H_8O_3$
crystal sizes	0.60 × 0.17 × 0.09	0.40 × 0.21 × 0.18	0.46 × 0.29 × 0.25
formula weight	146.14	162.20	188.17
space group	$Pc2_1b$	Pc	$P\bar{1}$
temperature/K	90.0(2)	90.0(2)	90.0(2)
unit cell dimensions			
a/Å	5.6091(13)	3.8056(3)	7.4772(15)
b/Å	7.7343(19)	8.4552(7)	9.6304(19)
c/Å	15.478(4)	11.3651(10)	11.989(2)
α/deg			85.751(11)
β/deg		95.629(4)	86.099(11)
γ/deg			81.753(11)
V/Å^3	671.5(3)	363.93(5)	850.6(3)
Z	4	2	4
D_c /g cm^{-1}	1.446	1.480	1.469
F(000)	394	168	392
absorption coeff/mm^{-1}	0.103	0.369	0.107
radiation	Mo Kα	Mo Kα	Mo Kα
$(\sin\theta/\lambda)_{max}$/Å^{-1}	1.08	1.08	1.08
reflections no. (unique)	6288	6373	12716
$R(F)$	0.0278	0.0158	0.0197
$R_w(F)$	0.0251	0.0145	0.0194
S	2.10	1.41	2.01
N_{obs}/N_{par}	14.68	20.14	12.71
range of residual density in asymmetric unit/e Å^{-3}	−0.241 to +0.174	−0.203 to +0.324	−0.194 to +0.224

to relate the charge density parameters at the BCP to local energy density $E(r_{CP})$ of the electrons by evaluating the local electronic kinetic energy density $G(r_{CP})$ and the local potential energy density $V(r_{CP})$ using the equations,[9,5,10]

$$G(r_{CP}) = \left(\frac{3}{10}\right)(3\pi^2)^{2/3}\rho^{5/3}(r_{CP}) + \left(\frac{1}{6}\right)\nabla^2\rho(r_{CP})$$

$$V(r_{CP}) = \left(\frac{1}{4}\right)\nabla^2\rho(r_{CP}) - 2G(r_{CP})$$

and

$$E(r_{CP}) = G(r_{CP}) + V(r_{CP})$$

The third condition refers to the value of the Laplacian at the BCP. The calculated values of $\nabla^2\rho_b(\mathbf{r})$ should be positive and should correlate with the interaction energy. The value of $\nabla^2\rho_b(\mathbf{r})$ should also agree with the range of values found so far in the literature. The fourth condition deals with the mutual penetration of the hydrogen and the acceptor atom. This condition, considered as necessary and sufficient, compares the nonbonded radii of the donor-hydrogen atom (r_D^0) and the acceptor atom (r_A^0) with their corresponding bonding radii. The nonbonding radius is taken to be equivalent to the gas-phase van der Waals radius of the participating atoms.[11] The bonding radius (r) is the distance from the nucleus to the BCP. In a typical hydrogen bond, the value of $\Delta r_D = (r_D^0 - r_D) > \Delta r_A = (r_A^0 - r_A)$ and $\Delta r_D + \Delta r_A > 0$ represent positive interpenetration. If either or both of these conditions are violated the interaction is essentially van der Waals in nature.

The rest of the four criteria are obtained from integration over the atomic basins of the participating H-atoms. The fifth condition states that the H-atom loses electrons resulting in an increased net charge on the H-atom. The sixth condition concerns the energetic destabilization of the H-atom strongly correlating with the fifth one. The difference in total energy between the crystal and the bare molecule should be positive. The seventh condition suggests a decrease of dipolar polarization (magnitude of the first moment, M) of the H-atom upon hydrogen bond formation. H-atomic volume depletion forms the basis for the eighth condition.

In an experimental charge density analysis on a series of ionic complexes, Mallinson et al. have evaluated both intra- and intermolecular interactions in terms of the first four criteria to demonstrate that there is a "Morse-like" dependence of the Laplacian, which allows to differentiate ionic and covalent bond character.[12] They conclude that the length of interaction line can be correlated with topological properties, which reveals a continuous transition from weak hydrogen bonding to strong covalent bonding situation. Further, they surmise that the penetration criterion is a sufficient condition to predict the presence or absence of a hydrogen bond and the four additional criteria, which invoke integration over the atomic basin, become expensive to calculate. However, restricting the integration to the basin of the participating H-atom only in terms of loss of charge, energy destabilization, decrease of dipolar polarization, and atomic volume would provide most of the characteristics of hydrogen bond formation.[7,8]

We have evaluated the nature of C−H···O and C−H···π interactions based on the experimental and theoretical charge density analyses on a series of compounds, 2*H*-chromen-2-one (coumarin), 2*H*-thiochromen-2-one (1-thiocoumarin), and 3-acetyl-2*H*-1-benzopyran-2-one (3-acetylcoumarin). The basic idea in choosing these two types of interactions is to allow the exploration of the region of the limit of a weak hydrogen bond as compared to a van der Waals interaction. Indeed, Koch and Popelier have compared C−H···O interactions with C−H···Cl interactions, which are considered weak van der Waals interactions.[7]

Coumarin has been extensively studied as it finds applications in several areas of synthetic chemistry, medicinal chemistry, and photochemistry. The formation of a [2+2] cycloaddition product upon irradiation[13] of coumarin and its derivatives has contributed immensely to the area of solid-state photochemistry. Several substituted coumarin derivatives find application in the dye industry[14,15] and in the area of LASER dyes[16] based on the property of these compounds showing state dependent variation in the static dipole moment. Coumarins have also been used to

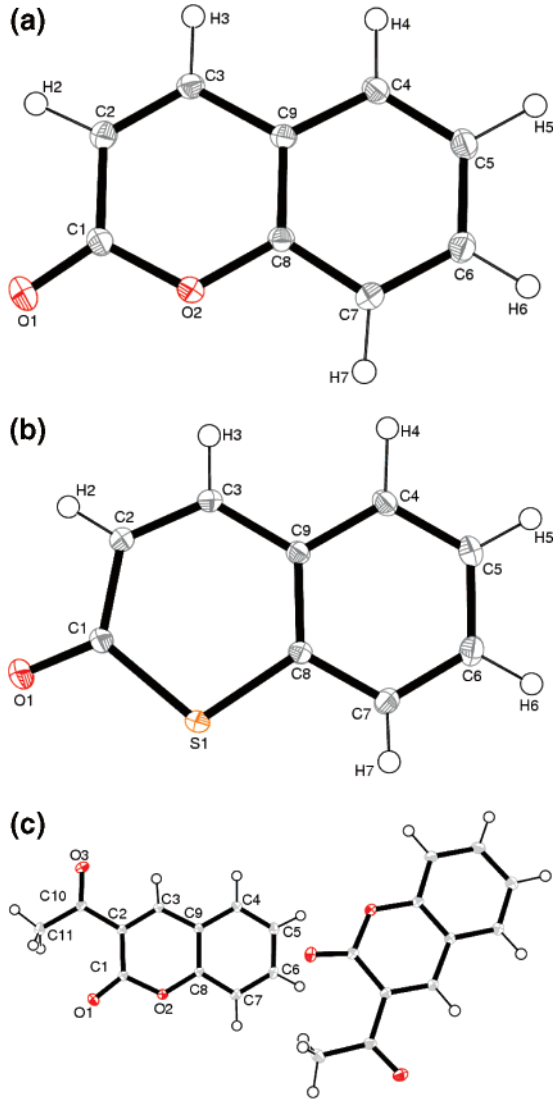

Figure 1. (a) ORTEP diagram with labels for atoms of coumarin at 90 K with 50% ellipsoid probability (non H-atoms). (b) ORTEP diagram with labels for atoms of 1-thiocoumarin at 90 K with 50% ellipsoid probability (non H-atoms). (c) ORTEP diagram with labels for atoms of 3-acetylcoumarin at 90 K with 50% ellipsoid probability (non H-atoms).

probe ultrafast solvation effects.[17] Coumarin and its sulfur derivatives possess well-defined dipole moments and exhibit second harmonic generation effects since they crystallize in noncentrosymmetric space groups.[18,19] We have studied the geometry and the molecular packing patterns of several coumarins and their derivatives[13] in order to evaluate the features of noncovalent interactions. We have earlier reported the charge density distribution in 2*H*-chromene-2-thione (2-thiocoumarin) and have evaluated the topological properties using the AIM approach.[20] The crystallographic details of the compounds studied here have already appeared elsewhere.[19,21,22] X-ray diffraction data at 90 K on all three compounds have been subjected to multipole atom refinements followed by the AIM approach to derive BCPs. The theoretical charge densitites including the periodicity in all the three crystals have been calculated using the DFT approach[23,24] based on the experimentally derived structural model.[25]

C−H···O interactions in crystal engineering have been shown to influence packing motifs,[26] and in a recent review Steiner comments that the understanding of weak hydrogen bonding is yet unclear.[27] Nishio and his group have analyzed the packing features of C−H···π interactions,[28−30] which bring out the features of such weak van der Waals interactions. Several charge density measurements have characterized[31−33] the nature of C−H···π interactions in terms of electron densities, BCPs, and Laplacians.

In this article, we have looked into the characterization of C−H···O and C−H···π interactions. Based on all eight of Koch and Popelier's criteria,[7] for the first time we have classified C−H···O interactions into two categories (hydrogen bonded and weak van der Waals interaction) and C−H···π interactions as weak van der Waals interactions.

Experimental Section

Quality crystals were grown by slow evaporation at ~8 °C in a refrigerator from a mixture of chloroform and *n*-hexane. The crystals of coumarin are colorless blocks, those of 1-thiocoumarin are pink blocks, and those of 3-acetylcoumarin are yellow prisms. The high-resolution single-crystal X-ray diffraction data were collected on a Bruker AXS SMART APEX CCD diffractometer using Mo Kα radiation (50 kV, 40 mA). To achieve the final temperature the ramp rate was set to 40 K/hr. During the data collection the temperature was maintained at 90.0(2) K by using the Oxford Cryo Systems with N_2 flows. Suitable crystals with reasonable sizes (Table 1) were mounted in a Lindeman capillary and allowed to stabilize at final temperature for an hour. The unit-cell parameters were determined repeatedly until the estimated standard deviations in cell dimensions did not vary beyond acceptable limits. The data were collected in three steps with different scan times (20, 40, and 60 s for coumarin and 1-thiocoumarin and 15, 55, and 105 s for 3-acetylcoumarin) to cover the full-sphere of reciprocal space with different 2θ settings of the detector (−25°, −50°, and −75°) and φ settings (0°, 90°, 180°, and 270°) of the goniometer. The scanning angle ω was set to 0.3° for each 606 frames. The crystal-to-detector distance was kept at 6.03 cm. This strategy[20] provides high resolution, large redundancy, and better completeness in data sets, which are the key factors for multipole refinement modeling. The data collection was monitored and reduced with the packages SMART[34] and SAINTPLUS,[34] respectively. Sorting, scaling, merging, and empirical correction for absorption of the set of intensities were performed with SORTAV.[35] The structures were solved by direct methods using SHELXS97[36] and refined in the spherical atom approximation (based on F^2) by using SHELXL97[36] as included in a complete package WinGX.[37] The molecular diagrams were generated using ORTEP.[38]

Multipole Refinement

The refinements were carried out with the module XDLSM incorporated in the software package XD.[39] The residual bonding density, not modeled in the conventional spherical refinement, is taken into account in this multipolar refinement. Scattering factors were derived from the Clementi and Roetti[40] wave functions for all atoms. The function minimized in the least-squares refinement is $\sum w(|F_0|^2 - K|F_c|^2)^2$ for all reflections with $I > 3\sigma(I)$. The same refinement procedure as described earlier by us[20] was followed in the present study. Initially only the scale factor was refined with all reflections. Next, to determine the accurate positional and thermal parameters the higher order ($\sin\theta/\lambda \geq 0.8$ Å^{-1}) refinements were performed for non-hydrogen atoms. The positional and isotropic thermal parameters of the H-atoms were then refined using the lower angle data ($\sin\theta/\lambda \leq 0.8$ Å^{-1}). Due to unavailability of the neutron data, the positions of the H-atoms in this refinement as well as in

TABLE 2: Intramolecular Bond Critical Points for All Three Compounds and Bond Ellipticity, $\epsilon = (\lambda_1/\lambda_2 - 1)$[a]

bond (A−B)	ρ_b	$\nabla^2\rho_b$	R_{ij}	$d1$ (A−CP)	$d2$ (CP−B)	λ_1	λ_2	λ_3	ϵ
				Coumarin					
O(1)−C(1)	3.297(36)	−40.688(184)	1.2171	0.7634	0.4537	−32.17	−29.27	20.76	0.10
	2.829	*−22.533*	*1.2171*	*0.7934*	*0.4237*	*−25.85*	*−23.85*	*27.17*	*0.08*
O(2)−C(1)	2.181(29)	−15.959(129)	1.3714	0.8125	0.5589	−19.18	−17.03	20.25	0.13
	1.996	*−17.904*	*1.3729*	*0.8315*	*0.5414*	*−15.81*	*−14.71*	*12.61*	*0.08*
O(2)−C(8)	2.035(28)	−13.581(123)	1.3730	0.8229	0.5501	−17.73	−16.16	20.31	0.10
	1.936	*−17.098*	*1.3724*	*0.8290*	*0.5434*	*−15.44*	*−13.85*	*12.19*	*0.12*
C(1)−C(2)	2.002(21)	−15.605(68)	1.4537	0.7694	0.6842	−15.59	−14.27	14.25	0.09
	1.902	*−15.371*	*1.4535*	*0.7674*	*0.6861*	*−13.57*	*−12.02*	*10.22*	*0.13*
C(3)−C(2)	2.372(21)	−22.128(69)	1.3522	0.6741	0.6781	−19.97	−15.88	13.73	0.26
	2.262	*−20.658*	*1.3527*	*0.6955*	*0.6573*	*−16.41*	*−13.59*	*9.34*	*0.21*
C(3)−C(9)	1.939(19)	−15.439(58)	1.4405	0.7598	0.6807	−15.61	−13.13	13.31	0.19
	1.944	*−15.817*	*1.4404*	*0.7239*	*0.7164*	*−13.49*	*−12.70*	*10.38*	*0.06*
C(4)−C(5)	2.280(24)	−20.503(74)	1.3881	0.7361	0.6520	−18.61	−16.16	14.27	0.15
	2.105	*−17.943*	*1.3883*	*0.6916*	*0.6967*	*−14.97*	*−12.92*	*9.94*	*0.16*
C(6)−C(5)	2.274(23)	−18.007(73)	1.4024	0.6679	0.7345	−17.69	−15.13	14.82	0.17
	2.077	*−16.845*	*1.4027*	*0.6978*	*0.7049*	*−14.55*	*−12.69*	*10.40*	*0.15*
C(7)−C(6)	2.255(22)	−18.865(67)	1.3905	0.6901	0.7005	−17.79	−15.24	14.16	0.17
	2.107	*−17.527*	*1.3905*	*0.6940*	*0.6966*	*−15.16*	*−12.55*	*10.18*	*0.21*
C(8)−C(7)	2.237(22)	−19.500(68)	1.3938	0.7169	0.6769	−18.34	−15.09	13.93	0.22
	2.115	*−19.135*	*1.3941*	*0.7460*	*0.6481*	*−15.82*	*−12.69*	*9.37*	*0.25*
C(8)−C(9)	2.206(18)	−20.611(56)	1.3999	0.7114	0.6885	−19.06	−14.90	13.35	0.28
	2.136	*−19.308*	*1.4003*	*0.7290*	*0.6713*	*−15.79*	*−13.21*	*9.69*	*0.20*
				1-Thiocoumarin					
S(1)−C(1)	1.359(38)	−2.076(45)	1.7736	0.9107	0.8628	−8.45	−6.72	13.09	0.26
	1.293	*−4.894*	*1.7715*	*0.9633*	*0.8082*	*−7.34*	*−6.19*	*8.64*	*0.19*
S(1)−C(8)	1.336(43)	−1.219(51)	1.7472	0.8771	0.8700	−8.24	−6.44	13.47	0.28
	1.401	*−6.132*	*1.7456*	*0.9596*	*0.7860*	*−7.99*	*−6.82*	*8.68*	*0.17*
O(1)−C(1)	2.979(16)	−23.635(83)	1.2229	0.7993	0.4236	−25.93	−24.50	26.79	0.06
	2.769	*−24.862*	*1.2241*	*0.7859*	*0.4381*	*−23.54*	*−22.24*	*20.92*	*0.06*
C(1)−C(2)	2.008(13)	−15.771(27)	1.4504	0.7208	0.7296	−14.94	−12.04	11.21	0.24
	1.894	*−14.336*	*1.4508*	*0.7666*	*0.6842*	*−13.46*	*−11.69*	*10.82*	*0.15*
C(2)−C(3)	2.401(15)	−22.244(31)	1.3578	0.6674	0.6904	−18.03	−14.09	9.88	0.28
	2.224	*−20.458*	*1.3558*	*0.6899*	*0.6659*	*−16.82*	*−13.35*	*9.71*	*0.26*
C(9)−C(3)	1.987(14)	−14.111(30)	1.4429	0.6981	0.7447	−14.52	−11.47	11.88	0.27
	1.901	*−15.085*	*1.4415*	*0.7188*	*0.7227*	*−13.86*	*−11.85*	*10.63*	*0.17*
C(9)−C(4)	2.184(14)	−17.383(31)	1.4110	0.7054	0.7056	−15.46	−13.42	11.50	0.15
	2.005	*−16.725*	*1.4103*	*0.7199*	*0.6904*	*−14.95*	*−12.13*	*10.36*	*0.23*
C(5)−C(4)	2.217(18)	−18.958(36)	1.3853	0.6747	0.7106	−17.03	−13.23	11.30	0.29
	2.130	*−18.644*	*1.3837*	*0.6816*	*0.7020*	*−16.01*	*−12.80*	*10.17*	*0.25*
C(6)−C(5)	2.241(17)	−18.632(39)	1.4015	0.6364	0.7651	−15.60	−13.54	10.51	0.15
	2.091	*−17.860*	*1.4019*	*0.6936*	*0.7084*	*−15.40*	*−12.94*	*10.48*	*0.19*
C(6)−C(7)	2.288(14)	−19.371(33)	1.3894	0.6759	0.7136	−16.49	−13.51	10.64	0.22
	2.111	*−17.845*	*1.3892*	*0.6812*	*0.7080*	*−15.49*	*−12.74*	*10.38*	*0.22*
C(8)−C(7)	2.308(13)	−20.965(31)	1.3998	0.7317	0.6681	−18.05	−13.71	10.79	0.32
	2.090	*−17.497*	*1.3984*	*0.7282*	*0.6702*	*−15.31*	*−12.61*	*10.42*	*0.21*
C(8)−C(9)	2.109(14)	−16.831(30)	1.4059	0.6632	0.7427	−15.38	−12.73	11.28	0.21
	2.037	*−16.982*	*1.4058*	*0.7175*	*0.6883*	*−14.96*	*−12.39*	*10.37*	*0.21*
				3-Acetylcoumarin					
O(1)−C(1)	3.144(15)	−35.318(95)	1.2093	0.7719	0.4375	−31.56	−26.93	23.17	0.17
	2.942	*−29.470*	*1.2095*	*0.7816*	*0.4279*	*−27.80*	*−25.28*	*23.61*	*0.10*
O(2)−C(1)	2.014(14)	−13.870(57)	1.3849	0.8117	0.5732	−16.86	−15.42	18.41	0.09
	1.895	*−15.726*	*1.3840*	*0.8342*	*0.5498*	*−14.99*	*−13.75*	*13.02*	*0.09*
O(2)−C(8)	2.090(14)	−16.342(58)	1.3667	0.8155	0.5511	−19.09	−15.20	17.95	0.26
	1.953	*−16.658*	*1.3662*	*0.8321*	*0.5342*	*−15.15*	*−14.04*	*12.53*	*0.08*
O(3)−C(10)	2.968(15)	−33.482(88)	1.2253	0.7751	0.4502	−29.32	−24.64	20.47	0.19
	2.796	*−26.739*	*1.2254*	*0.7914*	*0.4340*	*−24.76*	*−23.83*	*21.85*	*0.04*
O(1A)-C(1A)	3.109(14)	−35.690(85)	1.2132	0.7634	0.4498	−30.42	−25.00	19.73	0.22
	2.903	*−28.868*	*1.2134*	*0.7838*	*0.4296*	*−26.97*	*−24.87*	*22.97*	*0.08*
O(2A)-C(1A)	2.035(14)	−15.632(57)	1.3775	0.8196	0.5579	−17.97	−15.46	17.80	0.16
	1.930	*−17.107*	*1.3771*	*0.8364*	*0.5407*	*−15.46*	*−14.11*	*12.47*	*0.10*
O(2A)-C(8A)	2.003(14)	−14.055(57)	1.3694	0.8153	0.5540	−17.47	−14.62	18.03	0.19
	1.941	*−16.550*	*1.3687*	*0.8338*	*0.5348*	*−15.17*	*−13.85*	*12.47*	*0.10*
O(3A)-C10A	3.089(16)	−36.119(93)	1.2265	0.7735	0.4530	−30.66	−24.95	19.48	0.23
	2.812	*−28.524*	*1.2266*	*0.7897*	*0.4369*	*−25.15*	*−23.61*	*20.23*	*0.07*
C(2)−C(1)	1.911(9)	−15.302(29)	1.4660	0.7506	0.7155	−14.89	−13.09	12.69	0.14
	1.868	*−14.542*	*1.4657*	*0.6958*	*0.7699*	*−13.37*	*−11.77*	*10.59*	*0.14*
C(3)−C(2)	2.220(11)	−17.808(33)	1.3627	0.6867	0.6760	−16.99	−13.91	13.09	0.22
	2.233	*−20.159*	*1.3626*	*0.6865*	*0.6761*	*−16.43*	*−13.54*	*9.81*	*0.21*
C(3)−C(9)	1.911(10)	−13.264(30)	1.4338	0.7022	0.7316	−14.38	−12.13	13.24	0.19
	1.953	*−15.320*	*1.4338*	*0.7252*	*0.7086*	*−13.67*	*−12.42*	*10.77*	*0.10*
C(9)−C(4)	2.072(10)	−15.062(31)	1.4085	0.7308	0.6777	−15.83	−12.94	13.71	0.22
	2.043	*−17.344*	*1.4083*	*0.7166*	*0.6917*	*−15.01*	*−12.63*	*10.29*	*0.19*

TABLE 2 (Continued)

bond (A−B)	ρ_b	$\nabla^2\rho_b$	R_{ij}	$d1$ (A−CP)	$d2$ (CP−B)	λ_1	λ_2	λ_3	ϵ
				3-Acetylcoumarin					
C(4)−C(5)	2.176(10)	−16.478(32)	1.3930	0.7101	0.6829	−16.92	−13.21	13.65	0.28
	2.093	*−17.382*	*1.3929*	*0.7034*	*0.6895*	*−15.12*	*−12.69*	*10.43*	*0.19*
C(5)−C(6)	2.126(11)	−16.260(32)	1.4043	0.7268	0.6775	−16.11	−13.66	13.51	0.18
	2.066	*−17.450*	*1.4043*	*0.6985*	*0.7058*	*−15.11*	*−12.71*	*10.37*	*0.19*
C(7)−C(6)	2.162(11)	−17.653(33)	1.3901	0.6712	0.7189	−17.23	−13.62	13.19	0.26
	2.102	*−17.391*	*1.3901*	*0.7025*	*0.6877*	*−15.03*	*−12.76*	*10.40*	*0.18*
C(8)−C(7)	2.159(10)	−18.259(31)	1.3967	0.6974	0.6992	−17.30	−13.88	12.92	0.25
	2.111	*−18.611*	*1.3968*	*0.7289*	*0.6679*	*−15.64*	*−12.99*	*10.02*	*0.20*
C(8)−C(9)	2.157(10)	−18.883(36)	1.4007	0.7581	0.6427	−17.34	−13.98	12.44	0.24
	2.123	*−19.221*	*1.4004*	*0.7243*	*0.6760*	*−15.90*	*−13.25*	*9.93*	*0.20*
C(2)−C(10)	1.724(9)	−12.848(27)	1.5071	0.7632	0.7438	−13.50	−11.34	11.99	0.19
	1.730	*−12.269*	*1.5068*	*0.7504*	*0.7564*	*−12.20*	*−10.92*	*10.85*	*0.12*
C(10)−C(11)	1.700(9)	−9.498(22)	1.5003	0.7995	0.7008	−11.99	−10.92	13.42	0.10
	1.780	*−13.892*	*1.4999*	*0.7802*	*0.7197*	*−12.44*	*−11.88*	*10.43*	*0.05*
C(2A)-C(1A)	1.944(9)	−14.946(28)	1.4689	0.7390	0.7300	−15.33	−12.70	13.08	0.21
	1.874	*−14.887*	*1.4687*	*0.6943*	*0.7744*	*−13.65*	*−11.79*	*10.54*	*0.16*
C(2A)-C(3A)	2.233(11)	−17.393(33)	1.3625	0.7012	0.6613	−16.96	−13.73	13.30	0.24
	2.236	*−20.211*	*1.3628*	*0.6757*	*0.6871*	*−16.49*	*−13.53*	*9.80*	*0.22*
C(9A)-C(3A)	1.959(10)	−13.663(30)	1.4312	0.7221	0.7092	−14.55	−12.45	13.34	0.17
	1.956	*−15.300*	*1.4307*	*0.7067*	*0.7240*	*−13.66*	*−12.38*	*10.74*	*0.10*
C(9A)-C(4A)	2.070(10)	−15.956(30)	1.4096	0.7229	0.6868	−15.83	−13.41	13.29	0.18
	2.045	*−17.196*	*1.4095*	*0.7165*	*0.6930*	*−14.97*	*−12.57*	*10.35*	*0.19*
C(4A)-C(5A)	2.193(10)	−17.560(32)	1.3885	0.6939	0.6946	−16.84	−14.12	13.40	0.19
	2.105	*−17.663*	*1.3885*	*0.6965*	*0.6920*	*−15.11*	*−12.91*	*10.35*	*0.17*
C(5A)-C(6A)	2.146(11)	−16.356(32)	1.4064	0.6878	0.7186	−16.67	−13.33	13.65	0.25
	2.069	*−17.475*	*1.4064*	*0.6996*	*0.7068*	*−15.23*	*−12.70*	*10.46*	*0.20*
C(7A)-C(6A)	2.163(10)	−17.943(31)	1.3915	0.6885	0.7030	−16.89	−14.12	13.06	0.20
	2.090	*−17.573*	*1.3915*	*0.6924*	*0.6991*	*−15.08*	*−12.81*	*10.31*	*0.18*
C(8A)-C(7A)	2.184(10)	−19.204(33)	1.3925	0.7250	0.6675	−17.69	−14.11	12.60	0.25
	2.140	*−19.272*	*1.3924*	*0.7287*	*0.6637*	*−16.03*	*−13.14*	*9.90*	*0.22*
C(8A)-C(9A)	2.124(10)	−17.732(34)	1.4041	0.7462	0.6579	−16.95	−13.56	12.78	0.25
	2.098	*−18.527*	*1.4042*	*0.7292*	*0.6750*	*−15.55*	*−13.02*	*10.04*	*0.19*
C(2A)-C10A	1.707(9)	−11.189(28)	1.5026	0.7640	0.7387	−12.44	−11.33	12.58	0.10
	1.745	*−12.631*	*1.5025*	*0.7503*	*0.7522*	*−12.36*	*−11.09*	*10.82*	*0.11*
C10A−C11A	1.716(9)	−9.852(22)	1.5009	0.7925	0.7084	−12.01	−10.94	13.09	0.10
	1.756	*−13.218*	*1.5004*	*0.7817*	*0.7187*	*−12.12*	*−11.60*	*10.50*	*0.05*

[a] The values from periodic calculation using B3LYP/6-31G** method are given in italics.

the subsequent refinements were fixed to average bond distance values obtained from reported neutron diffraction studies[41] (C_{ar}−H = 1.08 Å and C_{methyl}−H = 1.06 Å). In the next stage of refinements releasing monopole, dipole, quadrupole, octapole, and hexadecapole populations with single κ were performed in a stepwise manner. Finally, a single κ' was refined for each species for all non H-atoms along with the rest of the parameters (including the isotropic thermal parameters of H-atoms). For all H-atoms, the multipole expansion was truncated at $l_{max} = 1$ (dipole, bond-directed) level, and for 1-thiocoumarin the sulfur atom was allowed to refine up to hexadecapole. For chemically different groups of non-hydrogen atoms, separate κ and κ' were allowed while for H-atoms the corresponding values were fixed at 1.2. No space group symmetry or chemical restraints were applied and the scale factor was allowed to refine throughout all refinements.

Theoretical Calculations

Calculation of Periodic Wave Function and Theoretical Structure Factors. The program *CRYSTAL03*[25] was used to perform the single-point periodic calculations based on the experimental geometry by using the density functional theory (DFT) method at the B3LYP[23,24] level with the 6-31G** basis set.[42] This basis set has been shown to provide reliable and consistent results with respect to studies involving intermolecular interactions.[33] The shrinking factors (IS1, IS2, and IS3) along the reciprocal lattice vectors were set at 4 (30 K-points in the irreducible Brillouin zone). For all the three compounds, the truncation parameters (ITOL), which control the accuracy of the calculation of the bielectronic Coulomb and exchange series, were set as ITOL1 = ITOL2 = ITOL3 = ITOL4 = 6 with ITOL5 = 17 for coumarin and 3-acetylcoumarin and ITOL5 = 15 for 1-thiocoumarin. Due to the large difference between ITOL4 and ITOL5, the exponents of the polarization functions were not scaled.[43] For faster convergence rate, the level shifter value was set equal to 0.3 hartree for coumarin and 3-actylcoumarin while for 1-thiocoumarin it is 0.5 hartree. Upon convergence on energy ($\sim 10^{-6}$) the periodic wave function was obtained and used to generate the theoretical structure factors with the option XFAC. Similar calculations at the Hartree−Fock (HF) level using the same basis set are under investigation.

Multipole Refinement and Topological Analysis. To eliminate an important source of correlation between parameters, the temperature factors and atomic positions were held fixed during the multipole refinement of the theoretical structure factors via XD. The same multipoles, as used in the refinement of experimental structure factors, were allowed to refine with separate κ' parameters for each non H-atom including all theoretical reflections. The module XDPROP[39] of the package XD was used for topological analysis of the electron density.

Evaluation of Atomic Basin Properties. Aicken and Popelier have described the details of atomic integration and the evaluation of atomic charges, electrostatic moments, volumes, and energies along with other atomic properties.[44] The module TOPXD[39] implemented in the package XD allows for the calculation of these properties in the crystal while the program

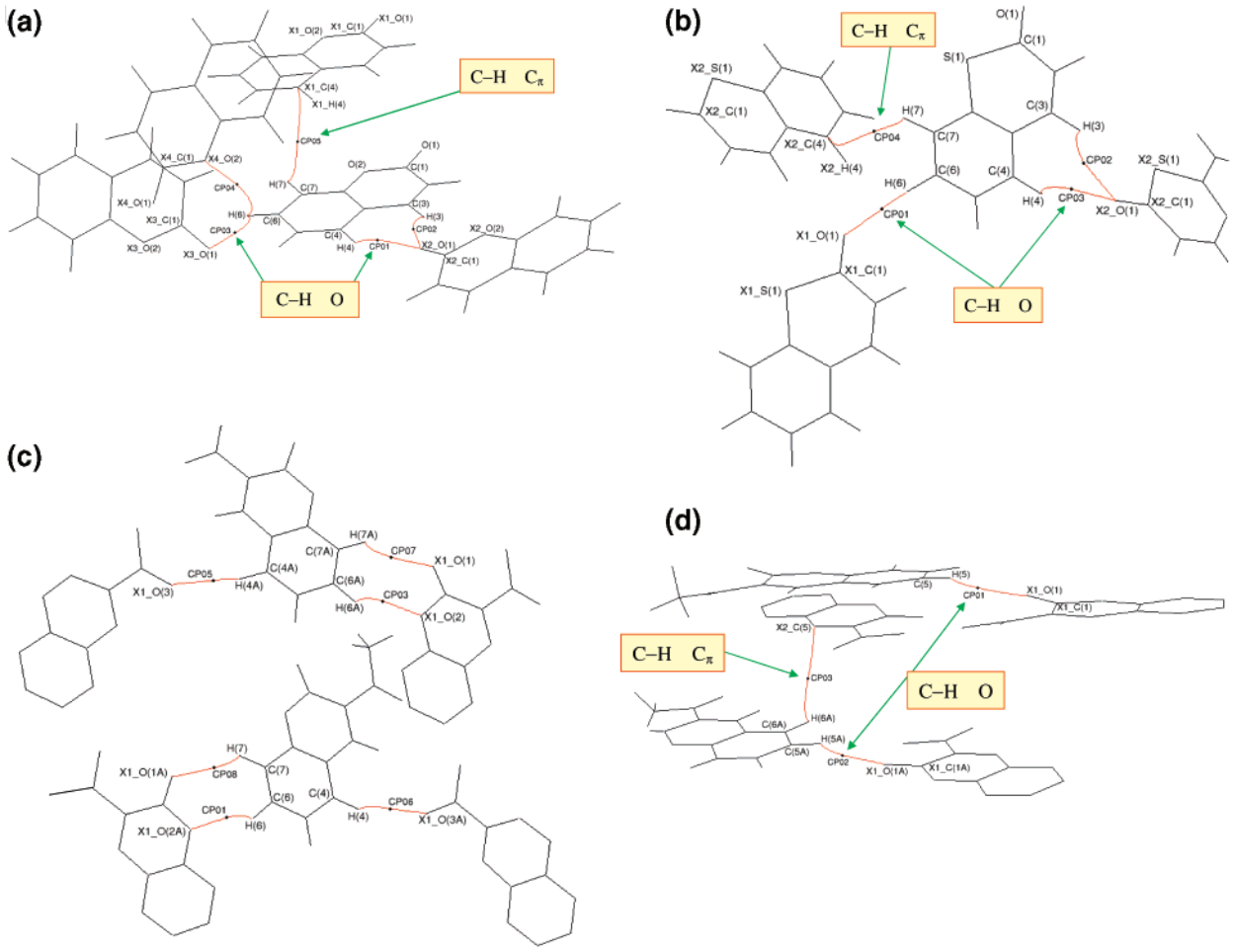

Figure 2. (a) Bond path character in coumarin showing the critical point locations along the C−H···O and C−H···C_π interactions shown in red. (b) Bond path character in 1-thiocoumarin showing the critical point locations along the C−H···O and C−H···C_π interactions shown in red. (c) Bond path character in 3-acetylcoumarin showing the critical point locations along the C−H···O interactions shown in red. (d) Bond path character in 3-acetylcoumarin showing the critical point locations along the C−H···O and C−H···C_π interactions shown in red.

MORPHY98[45] provides the corresponding information in the gas-phase for the isolated molecule. Ab initio geometry optimization and the corresponding wave functions for the isolated molecule were obtained via GAUSSIAN98,[46] both at the restricted HF and B3LYP levels with the 6-31G** basis set. In the calculations performed to evaluate the atomic basin properties both in the crystal and in the gas phase, similar values have been used for the integration variables. The HF level calculations have produced reliable atomic basin properties in several examples.[7,47,44] However, we have used the B3LYP/6-31G** level for the first time to calculate these properties to enable a direct comparison of the results between isolated molecule and theoretical crystal.

Results and Discussion

The unit cell parameters, the experimental details, and the multipole refinement parameters including the residual densities over the asymmetric unit for all the three compounds are listed in Table 1. Figure 1 gives the ORTEP diagrams of all the three compounds, showing the thermal ellipsoids at 50% probability level along with atom labeling. The final atomic coordinates, thermal parameters, bond lengths, and angles of all compounds are provided as Supporting Information. The bonds in all the three structures satisfy Hirshfeld's rigid bond test.[48] The largest differences of mean-square displacement amplitudes $\Delta_{A,B}$ for coumarin is 6×10^{-4} Å^2 for the bond C(4)−C(5), for 1-thiocoumarin it is 8×10^{-4} Å^2 for the S(1)−C(1) bond, and for 3-acetylcoumarin it is 6×10^{-4} Å^2 for the C(3)−C(9) bond. The experimental topological parameters of the covalent bonds within the molecule for all the three compounds along with the values obtained from periodic theoretical calculations are given in Table 2. It is noteworthy that the values obtained from experiment and theoretical calculations are in good agreement in all the three cases, with the maximum difference being 0.06, 0.03, and 0.08 Å for the C(6)−C(5) (1-thiocoumarin), C(1)−O(1) (coumarin), and C(8)−S(1) (1-thiocoumarin) bonds, respectively, in the location of the BCPs. The electron density and Laplacian values at the BCPs in each case are in good agreement, demonstrating that both experimental and theoretical methodologies provide comparative measures of topological and charge density properties. The C═O bond length and the associated BCPs differ in each case, which is a consequence of the nature of intermolecular interaction originating from the O-atom. Coumarin generates three C−H···O interactions in the crystal lattice, 1-thiocoumarin has also three C−H···O interactions, whereas 3-acetylcoumarin has an isolated C−H···O interaction at this O-atom. Figure 2 traces the bond paths (experimental) between O-atoms and the involved H-atoms with the (3, −1) BCPs along with representative bond path between C−H and the C_π for each compound. Representative Laplacian maps from experimental analysis showing the distribution in the region of the bond paths along C−H···O and C−H···C_π

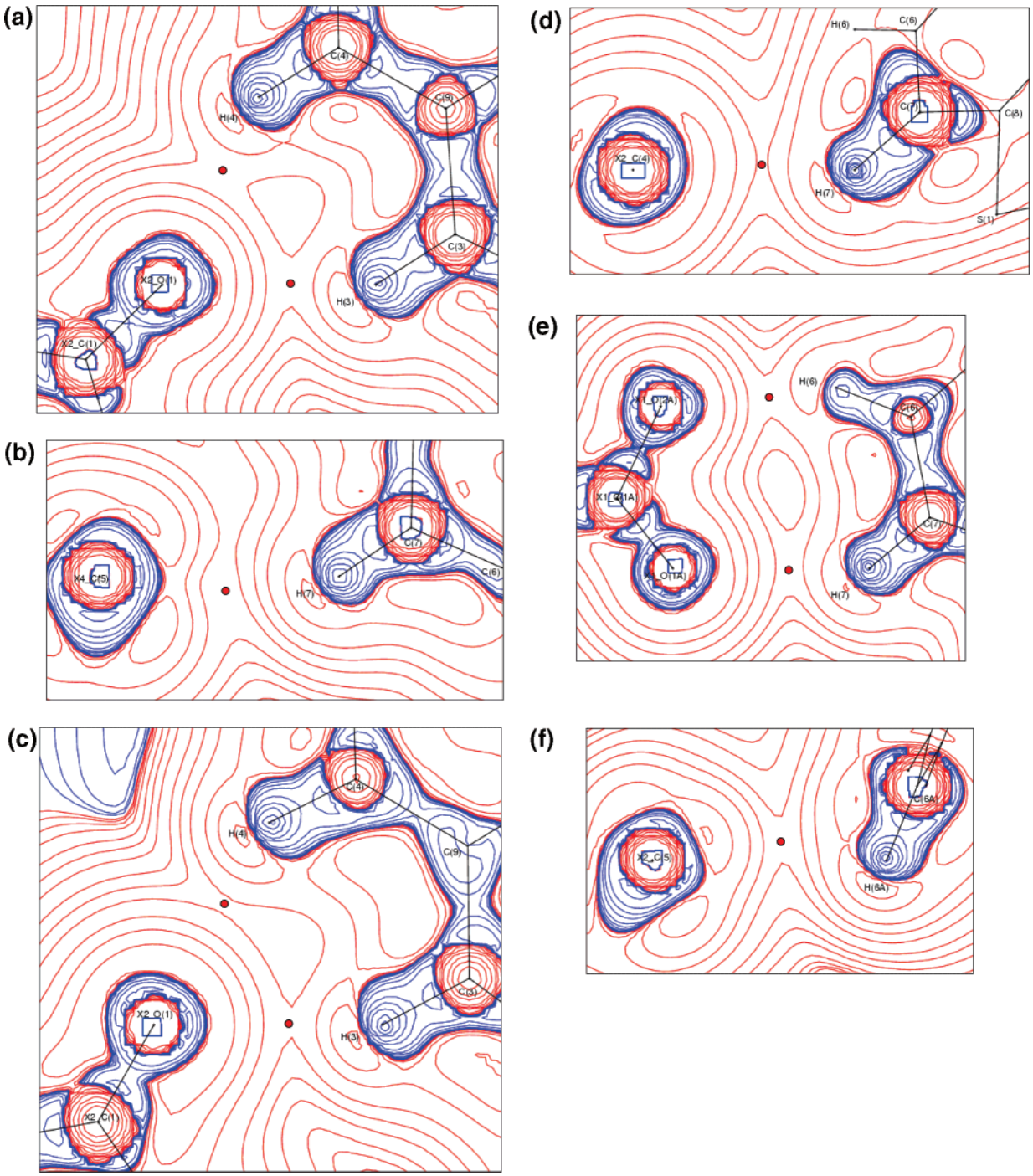

Figure 3. (a) Laplacian $[\nabla^2\rho_b(\mathbf{r})]$ of a representative C−H···O intermolecular interaction in coumarin. For all the Laplacian maps the contours are drawn at logarithmic intervals in $-\nabla^2\rho_b$ e Å^{-5}. Blue and red lines represent positive and negative contours, respectively. (b) Laplacian $[\nabla^2\rho_b(\mathbf{r})]$ of a representative C−H···C_π intermolecular interaction in coumarin. (c) Laplacian $[\nabla^2\rho_b(\mathbf{r})]$ of a representative C−H···O intermolecular interaction in 1-thiocoumarin. (d) Laplacian $[\nabla^2\rho_b(\mathbf{r})]$ of a representative C−H···C_π intermolecular interaction in 1-thiocoumarin. (e) Laplacian $[\nabla^2\rho_b(\mathbf{r})]$ of a representative C−H···O intermolecular interaction in 3-acetylcoumarin. (f) Laplacian $[\nabla^2\rho_b(\mathbf{r})]$ of a representative C−H···C_π intermolecular interaction in 3-acetylcoumarin.

are given in Figure 3. The corresponding theoretical maps are not shown in the figure since they display similar features. The multipole population parameters ($P_{lm\pm}$ and P_v) along with κ and κ' from experimental and theoretical refinements are provided as Supporting Information.

The main objectives of the present study is to characterize intermolecular interactions involving C−H···O and C−H···π in each structure and evaluate them based on all eight of Koch and Popelier's criteria. The C−H···π interactions considered for this study are limited to the aromatic carbon atom regions of the compounds. The details of all the parameters characterizing the interactions are given in Table 3. The inclusion of C−H···π interactions (van der Waals in nature) in our evaluation of the eight criteria arises from the fact that it provides an immediate comparison with a weak hydrogen bond such as C−H···O. Indeed C−H···O interactions define the possible limit of the hydrogen bond as can be seen in the evaluation of the eight criteria as follows. Thus these two interactions allow for the definition of a "region of overlap" between the hydrogen bond and a van der Waals interaction.

Criterion 1. BCPs and the linking bond paths are found in all interactions. The variation of electron density at the BCPs,

TABLE 3: Intermolecular Bond Critical Points and the Parameters Characterizing the Interactions[a]

interactions	R_{ij}	$\Delta r_D - \Delta r_A$	$\Delta r_D + \Delta r_A$	ρ_b	$\nabla^2\rho_b$	$G(r_{CP})$	$V(r_{CP})$
			Coumarin				
H(4)−X2−O(1)	2.434	0.121	0.306	0.045	0.915	18.39	−11.87
$(x+1, y-{}^1/_2, -z+{}^3/_2)$	*2.414*	*0.096*	*0.326*	*0.051*	*0.924*	*18.97*	*−12.78*
H(3)−X2−O(1)	2.310	0.123	0.230	0.036	0.775	15.30	−9.49
$(x+1, y-{}^1/_2, -z+{}^3/_2)$	*2.458*	*0.119*	*0.282*	*0.041*	*0.831*	*16.61*	*−10.59*
H(6)−X3−O(1)	2.725	−0.041	0.015	0.032	0.520	10.45	−6.74
$(-x, y, z-{}^1/_2)$	*2.698*	*−0.018*	*0.042*	*0.036*	*0.561*	*11.41*	*−7.55*
H(6)−X4−O(2)	2.834	−0.098	−0.094	0.033	0.518	10.47	−6.83
$(-x, y-{}^1/_2, -z+1)$	*2.771*	*−0.084*	*−0.031*	*0.035*	*0.552*	*11.19*	*−7.35*
H(5)−X4−C(8)	2.828	−0.046	−0.222	0.036	0.408	8.64	−6.16
$(-x+1, y-{}^1/_2, -z+1)$	*2.764*	*−0.042*	*0.286*	*0.031*	*0.438*	*8.91*	*−5.89*
H(7)−X4−C(5)	3.013	−0.086	0.037	0.027	0.237	5.06	−3.67
$(-x, y+{}^1/_2, -z+1)$	*2.993*	*−0.157*	*0.057*	*0.031*	*0.244*	*4.82*	*−2.99*
H(2)−X2−C(4)	3.021	−0.054	0.029	0.031	0.319	6.75	−4.81
$(x, y+{}^1/_2, -z+{}^3/_2)$	*3.009*	*−0.245*	*0.041*	*0.020*	*0.255*	*5.09*	*−3.24*
H(5)−X4−C(7)	3.057	−0.187	−0.007	0.025	0.239	5.01	−3.51
$(-x+1, y-{}^1/_2, -z+1)$	*3.042*	*−0.126*	*0.008*	*0.022*	*0.277*	*5.57*	*−3.60*
H(2)−X2−C(9)	3.131	−0.291	−0.081	0.015	0.229	4.44	−2.65
$(x, y+{}^1/_2, -z+{}^3/_2)$	*3.081*	*−0.331*	*−0.031*	*0.023*	*0.278*	*5.63*	*−3.69*
H(4)−X1−C(7)	3.150	−0.311	−0.100	0.014	0.200	3.89	−2.32
$(x+1, y, z)$	*3.156*	*−0.282*	*−0.106*	*0.021*	*0.244*	*4.82*	*−2.99*
H(7)−X1−C(4)	3.200	−0.262	−0.150	0.017	0.184	3.69	−2.37
$(x-1, y, z)$	*3.156*	*−0.435*	*−0.106*	*0.018*	*0.247*	*5.77*	*−3.63*
H(4)−X4−C(7)	3.208	−0.279	−0.158	0.025	0.211	4.50	−3.25
$(-x+1, y-{}^1/_2, -z+1)$	*3.134*	*−0.184*	*−0.084*	*0.022*	*0.253*	*5.13*	*−3.38*
H(7)−X1−C(5)	3.231	−0.066	−0.181	0.012	0.174	3.36	−1.97
$(x-1, y, z)$	*3.221*	*−0.286*	*−0.171*	*0.014*	*0.193*	*3.76*	*−2.26*
			1-Thiocoumarin				
H(6)−X1−O(1)	2.477	0.134	0.263	0.046	0.768	15.79	−10.67
$(x, y-1, z)$	*2.470*	*0.110*	*0.270*	*0.043*	*0.831*	*16.74*	*−10.85*
H(3)−X2−O(1)	2.555	0.198	0.185	0.024	0.680	12.97	−7.42
$(x, -y+2, z+{}^1/_2)$	*2.478*	*0.109*	*0.262*	*0.042*	*0.818*	*16.44*	*−10.60*
H(4)−X2−O(1)	2.603	0.144	0.137	0.027	0.590	11.47	−6.88
$(x, -y+2, z+{}^1/_2)$	*2.546*	*0.096*	*0.194*	*0.035*	*0.691*	*13.72*	*−8.62*
H(7)−X2−C(4)	2.832	−0.045	0.218	0.031	0.359	7.48	−5.17
$(x, -y+1, z-{}^1/_2)$	*2.847*	*−0.169*	*0.203*	*0.032*	*0.423*	*8.69*	*−5.86*
H(7)−X2−C(5)	2.987	−0.095	0.063	0.019	0.207	4.18	−2.73
$(x, -y+1, z-{}^1/_2)$	*3.015*	*−0.282*	*0.035*	*0.018*	*0.281*	*5.49*	*−3.32*
H(6)−X1−C(2)	3.048	−0.034	0.002	0.027	0.290	6.03	−4.15
$(x, y-1, z)$	*3.085*	*−0.230*	*−0.035*	*0.024*	*0.291*	*5.91*	*−3.89*
			3-Acetylcoumarin				
H(6)−X1−O(2A)	2.433	0.117	0.307	0.048	0.926	18.80	−12.37
$(x-1, y-1, z)$	*2.408*	*0.114*	*0.332*	*0.047*	*0.930*	*18.80*	*−12.27*
H(5A)−X1−O(1A)	2.442	0.188	0.298	0.038	0.927	18.18	−11.10
$(x, y-1, z)$	*2.427*	*0.141*	*0.313*	*0.042*	*0.868*	*17.35*	*−11.06*
H(6A)−X1−O(2)	2.445	0.128	0.295	0.044	0.885	17.78	−11.47
$(x+1, y, z)$	*2.408*	*0.110*	*0.332*	*0.048*	*0.933*	*18.92*	*−12.44*
H(5)−X1−O(1)	2.499	0.220	0.242	0.030	0.827	15.92	−9.32
$(x, y-1, z)$	*2.439*	*0.143*	*0.301*	*0.040*	*0.849*	*16.88*	*−10.63*
H(4A)−X1−O(3)	2.518	0.178	0.222	0.031	0.734	14.28	−8.58
$(x, y, z+1)$	*2.522*	*0.182*	*0.218*	*0.028*	*0.684*	*13.23*	*−7.83*
H(4)−X1−O(3A)	2.552	0.148	0.188	0.032	0.690	13.54	−8.28
$(x, y-1, z-1)$	*2.534*	*0.137*	*0.206*	*0.033*	*0.677*	*13.35*	*−8.27*
H(7A)−X1−O(1)	2.645	0.235	0.095	0.020	0.560	10.52	−5.79
$(x+1, y, z)$	*2.626*	*0.100*	*0.114*	*0.030*	*0.567*	*11.20*	*−6.96*
H(7)−X1−O(1A)	2.664	0.167	0.077	0.025	0.530	10.29	−6.15
$(x-1, y-1, z)$	*2.664*	*0.076*	*0.076*	*0.029*	*0.533*	*10.53*	*−6.55*
H(6A)−X2−C(5)	3.174	−0.230	−0.124	0.011	0.197	3.75	−2.13
$(-x+1, -y, -z)$	*3.162*	*−0.328*	*−0.112*	*0.016*	*0.223*	*4.37*	*−2.66*
H(6A)−X2−C(4)	3.177	−0.198	−0.127	0.014	0.248	4.76	−2.76
$(-x+1, -y, -z)$	*3.158*	*−0.338*	*−0.108*	*0.017*	*0.234*	*4.60*	*−2.83*
H(4A)−X2−C(3A)	3.189	−0.319	−0.139	0.013	0.220	4.22	−2.45
$(-x+1, -y+1, -z+1)$	*3.189*	*−0.319*	*−0.139*	*0.012*	*0.170*	*3.28*	*−1.94*
H(4)−X2−C(6A)	3.244	−0.312	−0.194	0.011	0.168	3.22	−1.87
$(-x+1, -y, -z)$	*3.244*	*−0.319*	*−0.194*	*0.015*	*0.188*	*3.70*	*−2.28*
H(6A)−X1−C(1)	3.381	0.117	−0.331	0.005	0.110	2.04	−1.09
$(x+1, y, z)$	*3.389*	*0.026*	*−0.339*	*0.007*	*0.117*	*2.20*	*−1.22*
H(6)−X1−C(7A)	3.382	0.312	−0.332	0.005	0.175	3.22	−1.68
$(x-1, y-1, z)$	*3.269*	*0.072*	*−0.218*	*0.013*	*0.194*	*3.75*	*−2.21*
H(6)−X1−C(1A)	3.409	0.109	−0.359	0.006	0.107	2.00	−1.10
$(x-1, y-1, z)$	*3.398*	*0.034*	*−0.348*	*0.006*	*0.114*	*2.13*	*−1.16*
H(5A)−X1−C(1A)	3.726	0.376	−0.676	0.005	0.106	1.97	−1.05
$(x, y-1, z)$	*3.600*	*0.302*	*−0.550*	*0.006*	*0.123*	*2.30*	*−1.24*
H(7A)−X2−C(1)	3.835	−0.373	−0.785	0.006	0.074	1.41	−0.80
$(-x+1, -y+1, -z)$	*3.842*	*−0.390*	*−0.792*	*0.005*	*0.070*	*1.32*	*−0.73*

[a] The values from periodic calculation using the B3LYP/6-31G** method are given in italics. The symmetry codes are given in the second row under each interaction.

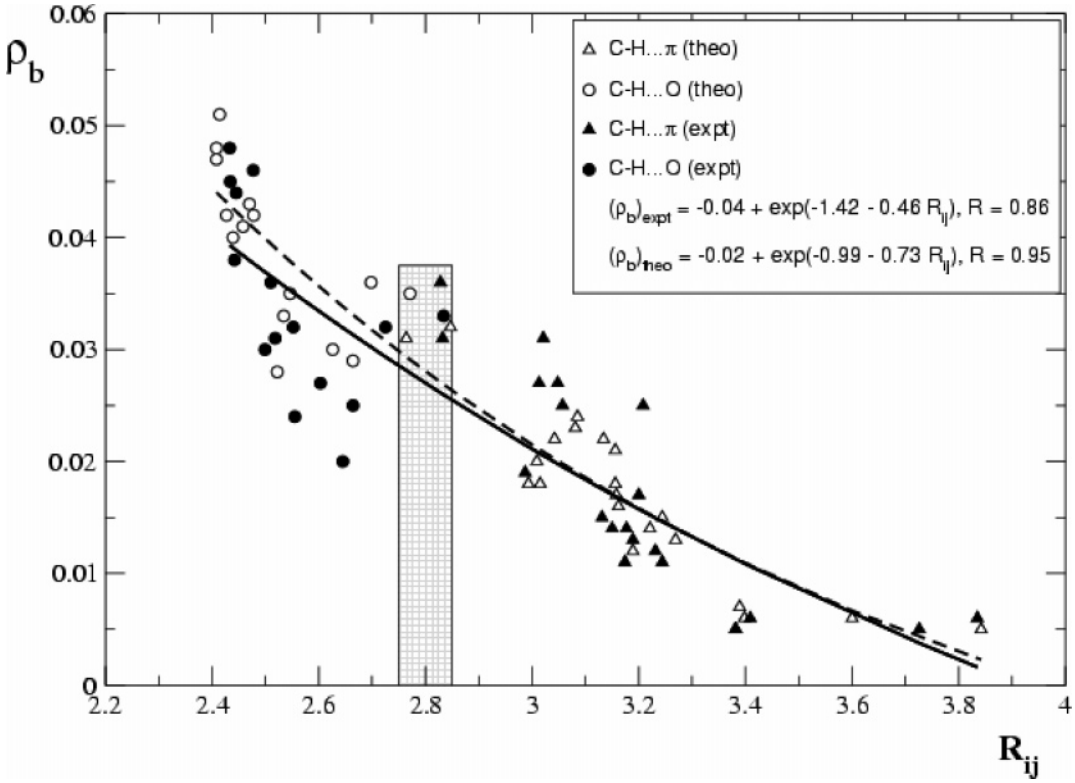

Figure 4. Exponential dependence of ρ_b [e Å^{-3}] on the interaction length R_{ij} [Å] for C−H···X (X = O or C$_\pi$) containing $N = 36$ data points (for all the hydrogen bonds in all three compounds). The solid and open symbols represent experimental and theoretical values, respectively. The inset gives the details of the fitting models (solid and broken lines represent experimental and theoretical fitting, respectively) along with correlation coefficients R.

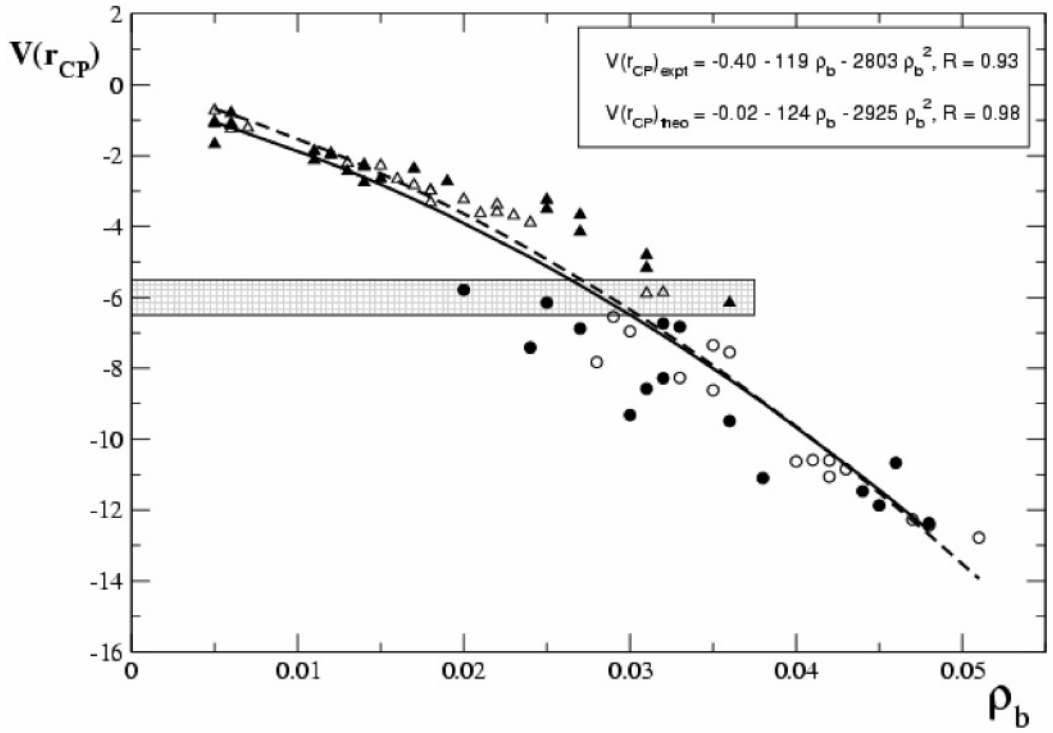

Figure 5. Quadratic relationship between local potential energy density $V(r_{CP})$ [kJ mol^{-1} bohr^{-3}] and ρ_b [e Å^{-3}] for $N = 36$ data points.

ρ_b, as a function of the length of the interaction line R_{ij} is shown in Figure 4. It is to be noted that the ρ_b values range from 0.005 to 0.048 e Å^{-3} (experiment), 0.005 to 0.051 e Å^{-3} (theory), and the corresponding R_{ij} values 2.433 to 3.835 Å (experiment) and 2.408 to 3.842 Å (theory). It is remarkable that even in this narrow range the dependence is analogous to Pauling's relation between bond orders and internuclear distances.[49−52] Most of the C−H···O hydrogen bonds reside in the range 2.4 to 2.7 Å for R_{ij}, while the C−H···π aggregates lie beyond 3 Å. The ρ_b values for C−H···O hydrogen bonds characteristically lie between 0.020 and 0.048 e Å^{-3} (experiment) and 0.028 to 0.051 e Å^{-3} (theory), and the corresponding ρ_b for C−H···π

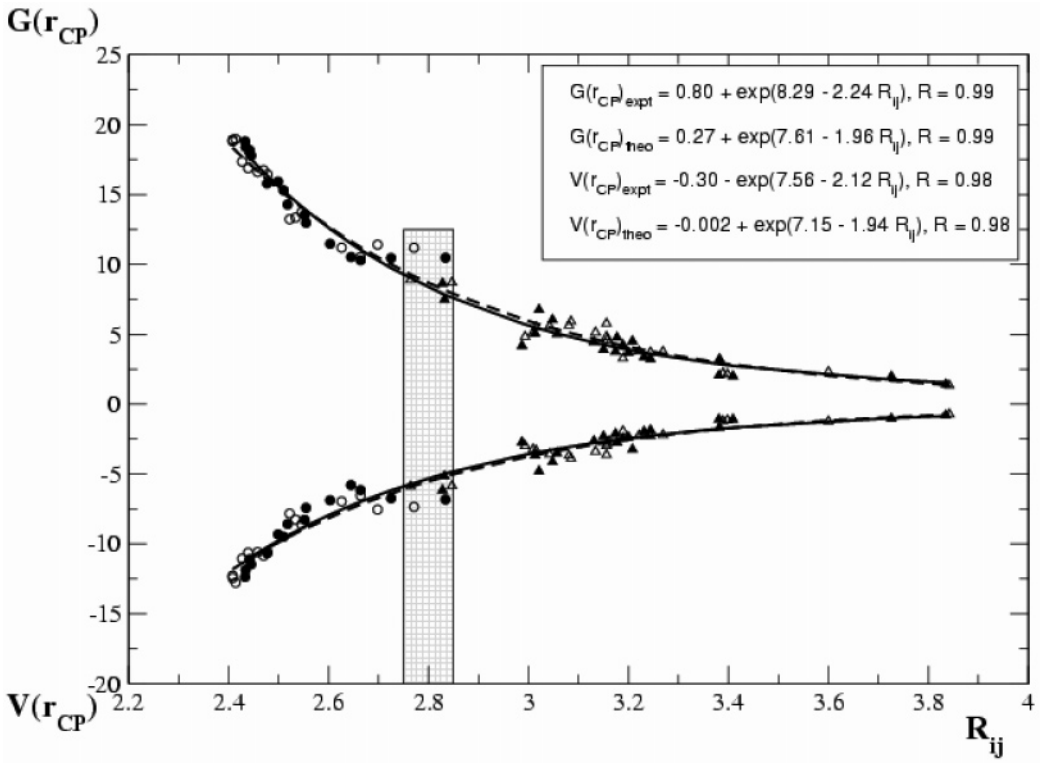

Figure 6. Exponential fitting of $V(r_{CP})$ [kJ mol^{-1} bohr^{-3}] and local kinetic energy density $G(r_{CP})$ [kJ mol^{-1} bohr^{-3}] values on R_{ij} [Å] for $N = 36$ data points.

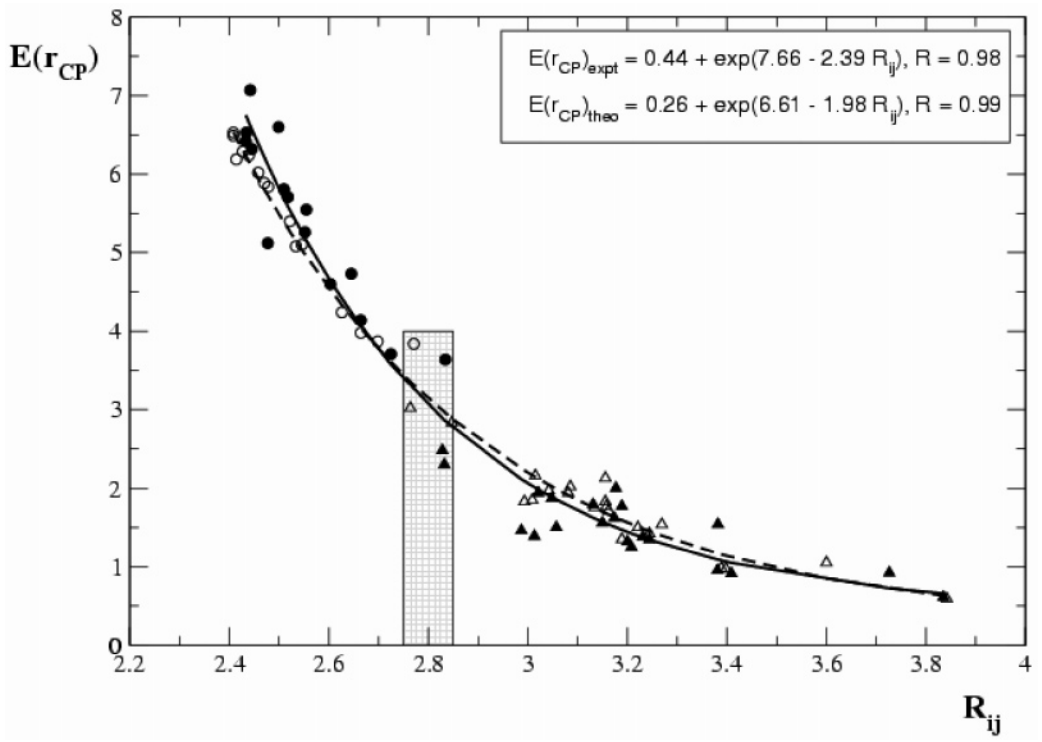

Figure 7. Exponential dependence of total local electron density $E(r_{CP})$ [kJ mol^{-1} bohr^{-3}] on R_{ij} [Å] for $N = 36$ data points.

interactions reside typically in the range 0.005 to 0.036 e Å^{-3} (experiment) and 0.005 to 0.032 e Å^{-3} (theory). Significantly, the shaded region in Figure 4 between the R_{ij} values of 2.75 to 2.85 Å contain representations from both C−H···O and C−H···π contacts, which we believe is a "region of overlap" between the hydrogen-bond and an interaction.

Criterion 2. In the experimental charge density studies we calculate the local potential energy density $V(r_{CP})$ at BCPs essentially to represent a quantity proportional to the hydrogen bond energy (Figure 5). The distribution fits a quadratic equation (curvilinear correlation coefficient, $R_{expt} = 0.93$ and $R_{theo} = 0.98$) similar to that observed by Mallinson et al. between strongest and weakest interactions.[12] Figure 5 clearly separates the C−H···O and C−H···π regions in the $V(r_{CP})$ ranges. Once again it is observed that the "region of overlap" delineates the hydrogen-bonding region with the interaction region as shown

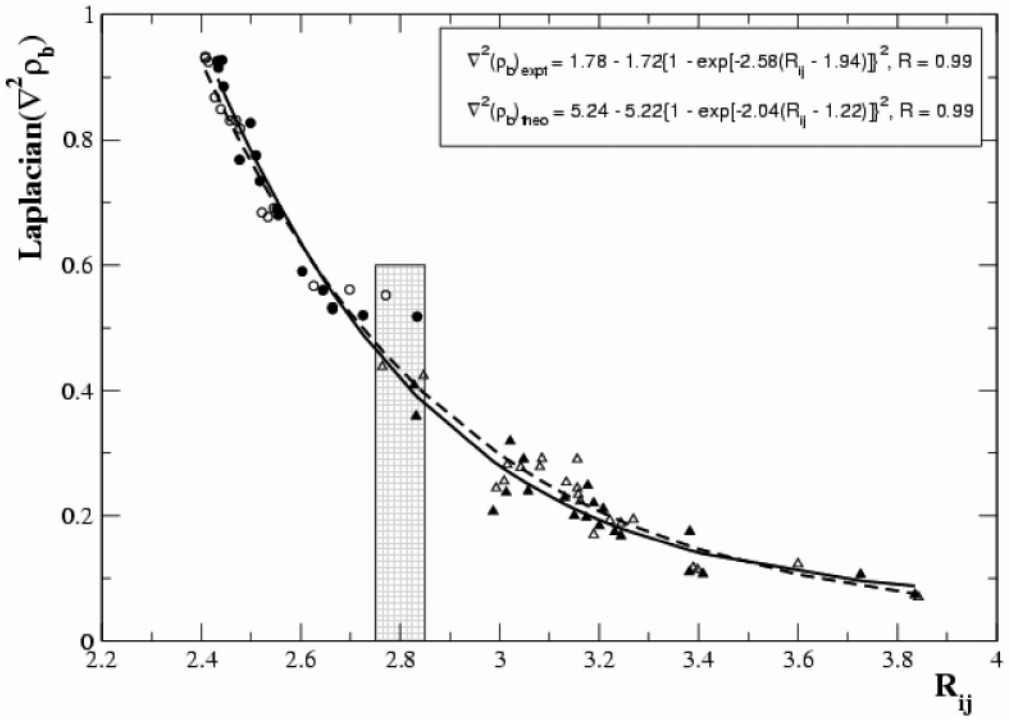

Figure 8. Morse-like dependence of Laplacian $[\nabla^2\rho_b(\mathbf{r})]$ (e Å^{-5}) on R_{ij} [Å] for $N = 36$ data points.

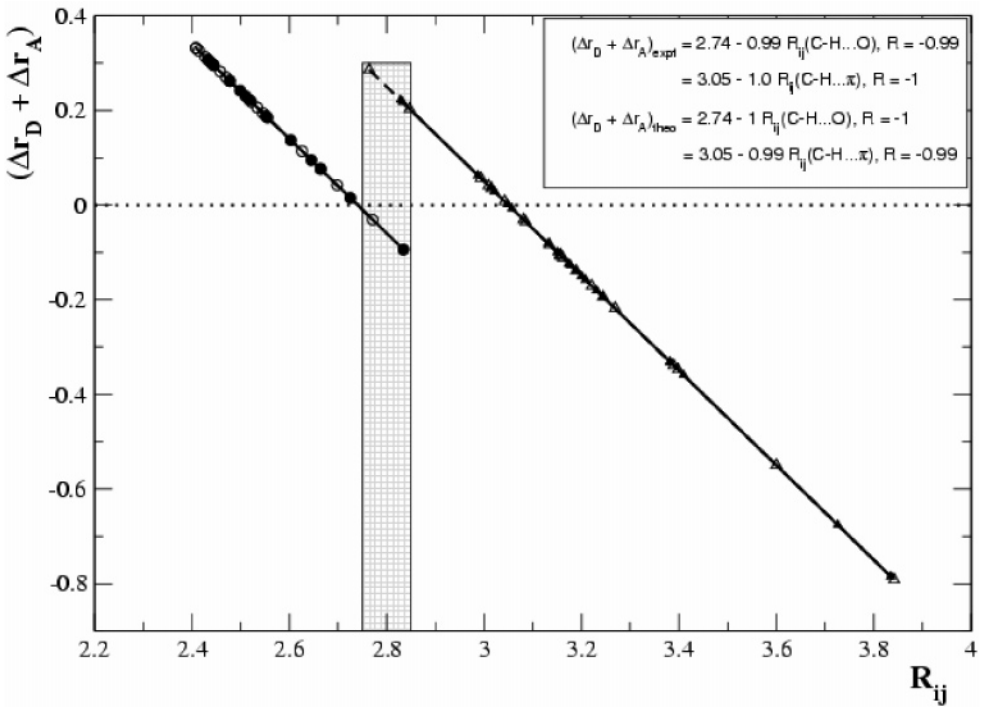

Figure 9. Linear dependence of $(\Delta r_D + \Delta r_A)$ [Å] on R_{ij} [Å] for $N = 15$ (C−H···O) and $N = 21$ (C−H···C_π) data points. The dotted line corresponds to $(\Delta r_D + \Delta r_A) = 0$.

by the shaded area. The corresponding $V(r_{CP})$ values are in the range of −5.5 to −6.5 kJ mol^{-1} bohr^{-3}. It is of interest to note that the theoretically derived values also lie in the same region, indicating a one-to-one correspondence between experiment and theory. Figure 6 shows the dependence of both the local kinetic and the potential energy densities [$V(r_{CP})$ and $G(r_{CP})$] on R_{ij}, which follows the expected exponential behavior. Figure 7 shows the exponential dependence of the total energy density [$E(r_{CP})$] on R_{ij}, and it resembles the dependence of ρ_b on R_{ij}.

Criterion 3. The relationship of Laplacian ($\nabla^2\rho_b$) and R_{ij} with the condition that $\nabla^2\rho_b$ should have positive values is depicted in Figure 8. The distribution resembles Morse-like, and the region of overlap is clearly demarked in the range 2.75 to 2.85 Å in R_{ij}. The Laplacian values range from 0.518 to 0.926 e Å^{-5} (experiment) and 0.533 to 0.933 e Å^{-5} (theory) for C−H···O interactions, while those of C−H···π are in the range 0.074 to 0.408 e Å^{-5} (experiment) and 0.070 to 0.438 e Å^{-5} (theory). It is to be noted that the values of the Laplacian lie in the range 0.35 to 0.55 e Å^{-5}, which defines the region of overlap.

Criterion 4. The nonbonded radii of the donor (r_D^0) and the acceptor (r_A^0) atoms are compared with their corresponding bonding radii. The quantity $\Delta r_D + \Delta r_A$ represents the inter-

TABLE 4: Atomic Net Charges (*q*), Atomic Potential Energy (*PE*), Atomic Dipolar Polarization (*M*), and Atomic Volume (*V*) of the H-Atoms in the Crystal and in the Isolated Molecule and Their Corresponding Differences (in au)

Atomic Net Charges (*q*)

		q (crystal)		*q* (isolated)		Δ*q* (crystal − isolated)			
interactions	atom	expt.(*E*)	theo.(*T*)	HF	DFT	E-HF	E-DFT	T-HF	T-DFT
				Coumarin					
C(4)...H(2)[a]	H(2)	0.2569	0.1080	0.0144	0.0441	0.2425	0.2128	0.0936	*0.0639*
C(9)...H(2)[a]									
O(1)...H(3)[b]	H(3)	0.0991	0.1280	−0.0083	0.0222	0.1074	0.0769	0.1291	*0.0986*
O(1)...H(4)[b]	H(4)	0.0957	0.0792	−0.0305	0.0074	0.1262	0.0883	0.1097	*0.0718*
C(7)...H(4)[c]									
C(7)...H(4)[d]									
C(7)...H(5)[e]	H(5)	0.0331	0.0655	−0.0317	0.0080	0.0648	0.0251	0.0972	*0.0575*
C(8)...H(5)[e]									
O(1)...H(6)[f]	H(6)	−0.0292	0.0859	−0.0241	0.0128	−0.0051	−0.0420	0.1100	*0.0731*
O(2)...H(6)[g]									
C(4)...H(7)[h]	H(7)	0.0662	0.0902	0.0026	0.0353	0.0636	0.0309	0.0876	*0.0549*
C(5)...H(7)[h]									
				1-Thiocoumarin					
O(1)...H(3)[i]	H(3)	0.0991	0.0980	−0.0164	0.0155	0.1155	0.0836	0.1144	*0.0825*
O(1)...H(4)[i]	H(4)	0.2872	0.1092	−0.0334	0.0058	0.3206	0.2814	0.1426	*0.1034*
O(1)...H(6)[j]	H(6)	0.3029	0.0809	−0.0250	0.0126	0.3279	0.29.3	0.1059	*0.0683*
C(2)...H(6)[j]									
C(4)...H(7)[k]	H(7)	0.2810	0.0561	−0.0193	0.0185	0.3003	0.2625	0.0754	*0.0376*
C(5)...H(7)[k]									

Atomic Potential Energy (*PE*)

		PE (crystal)		*PE* (isolated)		Δ*PE* (crystal − isolated)			
interactions	atom	expt.(*E*)	theo.(*T*)	HF	DFT	E-HF	E-DFT	T-HF	T-DFT
				Coumarin					
C(4)...H(2)	H(2)	−1.0446	−1.1936	−1.2514	−1.2189	0.2068	0.1743	0.0578	*0.0253*
C(9)...H(2)									
O(1)...H(3)	H(3)	−1.2564	−1.1901	−1.2733	−1.2368	0.0169	−0.0196	0.0832	*0.0467*
O(1)...H(4)	H(4)	−1.2461	−1.2245	−1.2916	−1.2486	0.0455	0.0025	0.0671	*0.0241*
C(7)...H(4)									
C(7)...H(4)									
C(7)...H(5)	H(5)	−1.3213	−1.2410	−1.2932	−1.2502	−0.0281	−0.0711	0.0522	*0.0092*
C(8)...H(5)									
O(1)...H(6)	H(6)	−1.4029	−1.2230	−1.2886	−1.2474	−0.1143	−0.1555	0.0656	*0.0244*
O(2)...H(6)									
C(4)...H(7)	H(7)	−1.2700	−1.2091	−1.2608	−1.2247	−0.0092	−0.0453	0.0517	*0.0156*
C(5)...H(7)									
				1-Thiocoumarin					
O(1)...H(3)	H(3)	−1.2408	−1.2098	−1.2865	−1.2461	0.0457	0.0053	0.0767	*0.0363*
O(1)...H(4)	H(4)	−1.0306	−1.2061	−1.2960	−1.2498	0.2654	0.2192	0.0899	*0.0437*
O(1)...H(6)	H(6)	−0.9684	−1.2293	−1.2887	−1.2454	0.3203	0.2770	0.0594	*0.1610*
C(2)...H(6)									
C(4)...H(7)	H(7)	−0.9787	−1.2526	−1.2837	−1.2400	0.3050	0.2613	0.0311	*−0.0126*
C(5)...H(7)									

Atomic Dipolar Polarization (*M*)

		M (crystal)		*M* (isolated)		Δ*M* (crystal − isolated)			
interactions	atom	expt.(*E*)	theo.(*T*)	HF	DFT	E-HF	E-DFT	T-HF	T-DFT
				Coumarin					
C(4)...H(2)	H(2)	0.0540	0.1006	0.0978	0.1209	−0.0438	−0.0669	0.0019	*−0.0203*
C(9)...H(2)									
O(1)...H(3)	H(3)	0.0251	0.0652	0.0972	0.1236	−0.0721	−0.0985	−0.0320	*−0.0584*
O(1)...H(4)	H(4)	0.0588	0.1013	0.0978	0.1258	−0.0390	−0.0670	0.0035	*−0.0245*
C(7)...H(4)									
C(7)...H(4)									
C(7)...H(5)	H(5)	0.0386	0.0768	0.0975	0.1237	−0.0589	−0.0851	−0.0207	*−0.0469*
C(8)...H(5)									
O(1)...H(6)	H(6)	0.0725	0.0969	0.0970	0.1230	−0.0245	−0.0505	−0.0001	*−0.0261*
O(2)...H(6)									
C(4)...H(7)	H(7)	0.1076	0.1126	0.0975	0.1218	0.0101	−0.0142	0.0151	*−0.0092*
C(5)...H(7)									
				1-Thiocoumarin					
O(1)...H(3)	H(3)	0.1033	0.0953	0.0986	0.1253	0.0047	−0.0220	−0.0033	*−0.0300*
O(1)...H(4)	H(4)	0.0478	0.0505	0.0978	0.1260	−0.0500	−0.0782	−0.0473	*−0.0755*
O(1)...H(6)	H(6)	0.1021	0.0743	0.0969	0.1230	0.0052	−0.0209	−0.0226	*−0.0487*
C(2)...H(6)									
C(4)...H(7)	H(7)	0.1561	0.0943	0.0971	0.1233	0.0590	0.0328	−0.0028	*−0.0290*
C(5)...H(7)									

TABLE 4 (Continued)

		Atomic Volume (V)							
		V (crystal)		V (isolated)		ΔV (crystal − isolated)			
interactions	atom	expt.(E)	theo.(T)	HF	DFT	E-HF	E-DFT	T-HF	T-DFT
				Coumarin					
C(4)...H(2)	H(2)	35.10	46.02	46.36	46.66	−11.26	−11.56	−0.34	*−0.64*
C(9)...H(2)									
O(1)...H(3)	H(3)	35.64	40.43	47.95	48.35	−12.31	−12.71	−7.52	*−7.92*
O(1)...H(4)	H(4)	38.64	41.84	48.89	49.12	−10.25	−10.48	−7.05	*−7.28*
C(7)...H(4)									
C(7)...H(4)									
C(7)...H(5)	H(5)	39.47	44.82	48.80	48.84	−9.33	−9.37	−3.98	*−4.02*
C(8)...H(5)									
O(1)...H(6)	H(6)	38.82	43.47	48.54	48.51	−9.72	−9.69	−5.07	*−5.04*
O(2)...H(6)									
C(4)...H(7)	H(7)	42.18	47.22	46.87	47.18	−4.69	−5.00	0.35	*0.04*
C(5)...H(7)									
				1-Thiocoumarin					
O(1)...H(3)	H(3)	34.45	41.27	47.44	47.96	−12.99	−13.51	−6.17	*−6.69*
O(1)...H(4)	H(4)	27.97	40.90	48.53	48.68	−20.56	−20.71	−7.63	*−7.78*
O(1)...H(6)	H(6)	34.80	43.28	48.54	48.52	−13.74	−13.72	−5.26	*−5.24*
C(2)...H(6)									
C(4)...H(7)	H(7)	38.90	45.16	47.94	48.06	−9.04	−9.16	−2.78	*−2.90*
C(5)...H(7)									

Symmetry codes: [a] $(x,y+1/2,-z+3/2)$, [b] $(x+1,y-1/2,-z+3/2)$, [c] $(x+1,y,z)$, [d] $(-x+1,y-1/2,-z+1)$, [e] $(-x+1,y-1/2,-z+1)$, [f] $(-x,y,z-1/2)$, [g] $(-x,y-1/2,-z+1)$, [h] $(x-1,y,z)$, [i] $(x,-y+2,z+1/2)$, [j] $(x,y-1,z)$, [k] $(x,-y+1,z-1/2)$.

penetration of van der Waals spheres of the donor and acceptor atoms. If this quantity has negative values, then the definition of hydrogen bond is not valid[7,8] even though there is a linear correlation between $\Delta r_D + \Delta r_A$ and R_{ij} (Figure 9). Further, if $\Delta r_D + \Delta r_A$ is also negative (Table 3), the interaction should be considered as van der Waals in nature. The differentiation between C−H···O and C−H···π is obvious in this figure and the limit of the hydrogen bond is well defined and corresponds to the R_{ij} values between 2.75 and 2.85 Å for the region of overlap. However, the overlap requirements do suggest possibilities of diffuseness in this region, as can be seen from the negative value of $\Delta r_D - \Delta r_A$ in case of the C(6)−H(6)···O(1) interaction in coumarin (Table 3).

Criteria 5−8. The evaluation of integrated properties over the basin of the H-atoms involved in the interactions forms the basis of these criteria. We have determined the charge, potential energy, dipolar polarization, and volume of H-atoms involved in the C−H···O and C−H···π interactions considering the crystal (experimental and theoretical) and the isolated molecule. The theoretical values have been calculated in the case of isolated molecules using both HF and DFT methods. Except in the case of 3-acetylcoumarin, where the calculations based on the isolated molecule indicate problems with optimization (values from experimental and theoretical calculation on crystal are given in Supporting Information, Table S26), we have compiled all the components of criteria 5−8 in Table 4. Since the theoretical calculation in the crystal is evaluated using only DFT, the integration properties appear most reliable with respect to the DFT calculation for isolated molecule and we have restrained the discussions to these values. A general trend emerges on inspection of Table 4 that the values for the C−H···O hydrogen bonds demarcate from the C−H···π van der Waals interactions. For example, the difference in charge on the H-atom increases from a value of 0.0549 *e* for C−H···π to a value of 0.0986 *e* for C−H···O hydrogen bond in the structure of coumarin. A similar trend is seen in case of 1-thiocoumarin with the values ranging from 0.0376 *e* to 0.0825 *e*, respectively. It is noteworthy that intermediate values are taken by those H-atoms, which display both C−H···π and C−H···O character. Comparable electron losses were found in case of formation of a dihydrogen bond[47] and also in a set of C−H···O bonds containing van der Waals complexes,[7] indicating that in general smaller electron loss reflects weak interaction. The differences in the potential energy (*PE*) in all cases depict the expected trend destabilizing the H-atom upon crystal formation. It is to be noted that calculations using TOPXD[39] give only the nuclear *PE* values, and hence for comparisons the kinetic energy output from the calculation on isolated molecules (MORPHY98[45]) is subtracted from the corresponding estimate of the total energy. The trends show that the increase in the *PE* for C−H···O hydrogen bond is larger compared to that in the C−H···π regime (for coumarin, 0.0467 au to 0.0092 au and for 1-thiocoumarin, 0.0363 au to −0.0126 au). The energy changes are strikingly significant in distinguishing between C−H···O hydrogen bond and C−H···π interaction. A measure of the extent and direction of dipolar polarization of the atomic electron density is given by the magnitude of the first moment, and this value decreases by 0.0584 au for the C−H···O bond and 0.0092 au for a C−H···π interaction in coumarin. The corresponding values for 1-thiocoumarin are 0.0755 au and 0.0290 au, respectively. The final criterion, decrease of H-atom's volume, is quite significant to bring in the difference in bond strength between the two types of interactions. The volume shrinks by 7.92 au for C−H···O as compared to 0.04 au for C−H···π interaction in coumarin while the values in 1-thiocoumarin are 7.78 au and 2.90 au, respectively. All these criteria show similar trends and allow distinguishing the two types of interactions on a quantitative footing.

Conclusion

Experimental and theoretical charge density calculation in three compounds belonging to the coumarin family suggests that there exists a well-defined "region of overlap" between hydrogen bond and van der Waals interaction. The lacuna of the identification of a lower limit for the hydrogen bond formation[27] has been addressed in our analysis. We believe that for the first time there is an experimental indication that at a critical distance X(donor)−H···A(acceptor) interaction is switched from "hydrogen bond" to "van der Waals" type. All eight of

Koch and Popelier's criteria[7] based on theoretical grounds are found necessary and sufficient to describe both qualitative and quantitative measures to evaluate the nature of C−H···O and C−H···π interactions. Further inputs from neutron diffraction studies, particularly to locate the position of hydrogen atoms unequivocally, would assist quantification of these results. However, the observed remarkable agreement between the theory and experiment is a sufficient indication to quantify the features of intermolecular interactions. These yardsticks form the tools of "quantitative crystal engineering", which allow for the identification of lower limit of a hydrogen bond.

Acknowledgment. P.M. thanks the CSIR, India, for a senior research fellowship. We thank DST-IRHPA, India, for the CCD facility at IISc., Bangalore. We are grateful to Professor P. R. Mallinson for his timely hints and advice.

Note Added after ASAP Publication. This paper was published ASAP on December 10, 2004, with some errors in the atom numbering and symmetry codes in Table 3 (section for 3-Acetylcoumarin). The corrected version was posted January 6, 2005.

Supporting Information Available: Fractional atomic coordinates, anisotropic displacement parameters, bond lengths, angles, multipole population coefficients, and κ and κ' values obtained from the multipole refinement and definitions of local axes. This material is available free of charge via the Internet at http://pubs.acs.org.

References and Notes

(1) Coppens, P. *Acta Crystallogr.* **1998**, *A54*, 779−788.
(2) Coppens, P. *X-ray Charge Densities and Chemical Bonding*, Oxford University Press: Oxford, 1997.
(3) Koritsanszky, T. S.; Coppens, P. *Chem. Rev.* **2001**, *101*, 1583−1621.
(4) Hansen, N. K.; Coppens, P. *Acta Crystallogr*. **1978**, *A34*, 909.
(5) Bader, R. F. W. *Atoms in Molecules: A Quantum Theory*; Oxford University Press: Oxford, U.K. 1990.
(6) Bader, R. F. W. *J. Phys. Chem. A* **1998**, *102*, 7314−7323.
(7) Koch, U.; Popelier, P. L. A. *J. Phys. Chem.* **1995**, *99*, 9747−9754.
(8) Popelier, P. *Atoms in Molecules. An Introduction*; Prentice Hall: U.K., 2000; pp 150−153.
(9) Abramov, Yu. A. *Acta Crystallogr*. **1997**, *A53*, 264−272.
(10) Espinosa, E.; Molins, E.; Lecomte, C. *Chem. Phys. Lett.* **1998**, *285*, 170−173.
(11) (a) Bondi, A. *J. Phys. Chem.* **1964**, *68*, 441−451. (b) Nyburg, S. C.; Faerman, C. H. *Acta Crystallogr.* **1985**, *B41*, 274−279.
(12) Mallinson, P. R.; Smith, G. T.; Wilson, C. C.; Grech, E.; Wozniak, K. *J. Am. Chem. Soc.* **2003**, *125*, 4259−4270.
(13) Vishnumurthy, K.; Guru Row, T. N.; Venkatesan, K. In *Molecular and Supramolecular Photochemistry*; Ramamurthy, V., Schanze, K. S., Eds.; Marcel Dekker: New York, 2001; Vol. 8, pp 427−460.
(14) Hooper, D. C.; Wolfson, J. S.; McHugh, G. L.; Winters, M. B.; Swartz, M. N. *Antimicrob. Agents Chemother.* **1982**, *22*, 662−671.
(15) Morris, A.; Russell, A. D. *Prog. Med. Chem.* **1971**, *8*, 39−59.
(16) (a) Nemkovich, N. A.; Reis, H.; Baumann, W. *J. Lumin.* **1997**, *71*, 255−263 and the references therein. (b) Khalfan, H.; Abuknesha, R.; Rond-Weaver, M.; Price, R. G.; Robinson, R. *Chem. Abstr.* **1987**, *106*, 63932.
(17) Maroncelli, M.; Fleming, G. R. *J. Chem. Phys.* **1987**, *86*, 6221−6239.
(18) Munshi, P.; Guru Row, T. N. *Acta Crystallogr*. **2001**, *E57*, o1175−o1176.
(19) Munshi, P.; Guru Row, T. N. *Acta Crystallogr*. **2002**, *E58*, o353−o354.
(20) (a) Munshi, P.; Guru Row, T. N. *Acta Crystallogr*. **2002**, *B58*, 1011−1017. (b) Munshi, P.; Guru Row, T. N. *Acta Crystallogr*. **2003**, *B59*, 159.
(21) Myasnikova, R. M.; Davydova, T. S.; Simonov, V. I. *Kristallografiya*. **1973**, *18*, 720−724.
(22) Munshi, P.; Venugopala, K. N.; Jayashree, B. S.; Guru Row, T. N. *Cryst. Growth Des.* **2004**, *4* (6), 1105−1107.
(23) Becke, A. D. *J. Chem. Phys.* **1993**, *98*, 5648−5652.
(24) Lee, C.; Yang, W.; Parr, R. G. *Phys. Rev. B* **1988**, *37*, 785−789.
(25) Saunders, V. R.; Dovesi, R.; Roetti, C.; Causa, M.; Harrison, N. M.; Orlando, R.; Zicovich-Wilson, C. M. CRYSTAL03 1.0 User's Manual, 2003.
(26) (a) Desiraju, G. R. *Acc. Chem. Res.* **1991**, *24*, 290−296. (b) Aakeroy, C. B.; Sneddon, K. R. *Chem. Soc. Rev.* **1993**, *22*, 397−407. (c) Desiraju, G.; Kashino, S.; Coombs, M. M.; Glusker, J. *Acta Crystallogr.* **1993**, *B49*, 880−892.
(27) Steiner, T. *Crystallogr. Rev.* **2003**, *9*, 177−228.
(28) (a) Umezawa, Y.; Tsuboyama, S.; Honda, K.; Uzawa, J.; Nishio, M. *Bull. Chem. Soc. Jpn.* **1998**, *71*, 1207−1213. (b) Umezawa, Y.; Tsuboyama, S.; Takahashi, H.; Uzawa, J.; Nishio, M. *Tetrahedron* **1999**, *55*, 10047−10056.
(29) Nishio, M.; Hirota, M.; Umezawa, Y. *The CH/pi Interaction. Evidence, Nature, and Consequences*; Wiley-VCH: New York, 1998.
(30) Nishio, M. *Cryst. Eng. Commun.* **2004**, *6*, 130−158.
(31) Mallinson, P. R.; Wozniak, K.; Wilson, C. C.; McCormac, K. L.; Yufit, D. S. *J. Am. Chem. Soc.* **1999**, *121*, 4640−4646.
(32) Ellena, J.; Goeat, A. E.; Howard, J. A. K.; Punte, G. *J. Phys. Chem.* **2001**, *105*, 8696−8708 and references therein.
(33) Oddershede, J.; Larsen, S. *J. Phys. Chem. A* **2004**, *108*, 1057−1063.
(34) SMART (V5.628), SAINT (V6.28); Bruker AXS Inc.: Madison, Wisconsin, 1998.
(35) Blessing, R. H. *Crystallogr. Rev.* **1987**, *1*, 3−58.
(36) Sheldrick, G. M. SHELXS97 and SHELXL97 programs for crystal structure refinement, University of Göttingen, Germany, 1997.
(37) Farrugia, L. J. WinGX (Version 1.64.05). *J. Appl. Crystallogr.* **1999**, *32*, 837−838.
(38) Farrugia, L. J. *J. Appl. Crystallogr.* **1997**, 30, 565.
(39) Koritsanszky, T. S.; Howard, S.; Macchi, P.; Gatti, C.; Farrugia, L. J.; Mallinson, P. R.; Volkov, A.; Su, Z.; Richter, T.; Hansen, N. K. XD (version 4.10, July), a computer program package for multipole refinement and analysis of electron densities from diffraction data. Free University of Berlin, Germany; University of Wales, Cardiff, UK.; Università di Milano, U.K.; CNR−ISTM, Milano, U.K.; University of Glasgow, U.K.; State University of New York, Buffalo, ; University of Nancy, France, 2003.
(40) Clementi, E.; Roetti, C. *Atomic Data and Nuclear Data Tables* **1974**, *14*, 177−478.
(41) Allen, F. H. *Acta Crystallogr*. **1986**, *B42*, 515−522.
(42) Hariharan, P. C.; Pople, J. A. *Theor. Chim. Acta* **1973**, *28*, 213−222.
(43) Spackman, M. A.; Mitchell, A. M. *Phys. Chem. Chem. Phys.* **2001**, *3*, 1518−1523.
(44) Aicken, F. M.; Popelier P. L. A. *Can. J. Chem.* **2000**, *78*, 415−426.
(45) MORPHY98, a program written by P. L. A. Popelier with a contribution from R. G. A. Bone, UMIST: Manchester, U.K., EU, 1998.
(46) Frisch, M. J.; Trucks, G. W.; Schlegel, H. B.; Scuseria, G. E.; Robb, M. A.; Cheeseman, J. R.; Zakrzewski, V. G.; Montgomery, J. A., Jr.; Stratmann, R. E.; Burant, J. C.; Dapprich, S.; Millam, J. M.; Daniels, A. D.; Kudin, K. N.; Strain, M. C.; Farkas, O.; Tomasi, J.; Barone, V.; Cossi, M.; Cammi, R.; Mennucci, B.; Pomelli, C.; Adamo, C.; Clifford, S.; Ochterski, J.; Petersson, G. A.; Ayala, P. Y.; Cui, Q.; Morokuma, K.; Malick, D. K.; Rabuck, A. D.; Raghavachari, K.; Foresman, J. B.; Cioslowski, J.; Ortiz, J. V.; Stefanov, B. B.; Liu, G.; Liashenko, A.; Piskorz, P.; Komaromi, I.; Gomperts, R.; Martin, R. L.; Fox, D. J.; Keith, T.; Al-Laham, M. A.; Peng, C. Y.; Nanayakkara, A.; Gonzalez, C.; Challacombe, M.; Gill, P. M. W.; Johnson, B.; Chen, W.; Wong, M. W.; Andres, J. L.; Gonzalez, C.; Head-Gordon, M.; Replogle, E. S.; Pople, J. A. *GAUSSIAN 98*; Gaussian, Inc.: Pittsburgh, PA, 1998.
(47) Popelier, P. L. A. *J. Phys. Chem. A* **1998**, *102*, 1873−1878.
(48) Hirshfeld, F. L. *Acta Crystallogr.* **1976**, *A32*, 239−244.
(49) Mallinson, P. R.; Wozniak, K.; Smith, G. T.; McCormac, K. L. *J. Am. Chem. Soc.* **1997**, *119*, 11502−11509.
(50) Espinosa, E.; Souhassou, M.; Lachekar, H.; Lecomte, C. *Acta Crystallogr*. **1999**, *B55*, 563−572.
(51) Espinosa, E.; Alkorta, I.; Elguero, J.; Molins, *J. Chem. Phys.* **2002**, *117*, 5529−5542.
(52) Pauling, L. *The Nature of the Chemical Bond*; Cornell University Press: Ithaca, New York, 1960.